

Arginine methylation of G3BP1 in response to Wnt3a regulates β -catenin mRNA

Rama Kamesh Bikkavilli* and Craig C. Malbon

Department of Pharmacology, School of Medicine, Health Sciences Center, State University of New York at Stony Brook, Stony Brook, NY 11794-8651, USA

*Author for correspondence (kamesh@pharm.stonybrook.edu)

Accepted 7 March 2011

Journal of Cell Science 124, 2310-2320

© 2011. Published by The Company of Biologists Ltd

doi:10.1242/jcs.084046

Summary

Wnt/ β -catenin signaling is essential for normal mammalian development. Wnt3a activates the Wnt/ β -catenin pathway through stabilization of β -catenin; a process in which the phosphoprotein Dishevelled figures prominently. Protein arginine methylation in signaling complexes containing Dishevelled was investigated. Mass spectrometry of a prominent arginine-methylated, Dishevelled-associated protein identified the Ras GTPase activating protein-binding protein 1 G3BP1. Stimulation of totipotent mouse embryonic F9 cells with Wnt3a provoked increased methylation of G3BP1. We show that G3BP1 is a novel *Cttnb1* mRNA binding protein. Methylation of G3BP1 constitutes a molecular switch that regulates *Cttnb1* mRNA in response to Wnt3a. Thus, the protein arginine methylation that targets G3BP1 acts as a novel regulator of *Cttnb1* mRNA.

Key words: Wnt, β -catenin mRNA, G3BP1, Arginine methylation, Dishevelled, Frizzled, RNA binding protein, Protein arginine methyl transferase

Introduction

Wnt/ β -catenin signaling has an essential role in mammalian development and its deregulation leads to human carcinomas (Polakis, 2000; Moon et al., 2002; Logan and Nusse, 2004; Moon et al., 2004; Angers and Moon, 2009). Wnt ligands bind to Frizzled proteins (Bhanot et al., 1996; Liu et al., 2001), which are G-protein coupled receptors (GPCRs) that are necessary for downstream signaling. Wnts regulate both canonical (Wnt/ β -catenin) as well as non-canonical (planar cell polarity and Wnt, cyclic GMP and Ca^{2+}) pathways (Bhanot et al., 1996; Liu et al., 1999). In the canonical pathway and in the absence of Wnt, β -catenin is regulated at the level of both mRNA and protein. At the mRNA level, the phosphoprotein scaffold Dishevelled3 in complex with the KH type-splicing regulatory protein KSRP promotes destabilization of mRNA encoding β -catenin (*Cttnb1*) (Bikkavilli and Malbon, 2010). At the protein level, β -catenin is degraded by the proteasome-dependent destruction complex, which is composed of several proteins. Axin and APC (the product of the adenomatous polyposis coli gene), for example, facilitate the phosphorylation of β -catenin by the Ser/Thr protein kinase glycogen synthase kinase 3 β (GSK3 β). GSK3 β -catalyzed phosphorylation provokes ubiquitylation and proteasome-mediated degradation of β -catenin. Wnt3a acts to oppose the ability of the Dishevelled3 (Dvl3)–KSRP complex to destabilize *Cttnb1* mRNA, as well as degradation of β -catenin, which is catalyzed by GSK3 β phosphorylation. The ability of Wnt to enhance post-transcriptional stabilization of *Cttnb1* mRNA, followed by translation (Bikkavilli and Malbon, 2010) and reduced protein degradation, stimulates rapid accumulation of intracellular β -catenin. Accumulation of β -catenin provokes its translocation into the nucleus, stimulating activation

of lymphoid enhancer factor and T cell factor (Lef/Tcf)-sensitive gene transcription (Behrens et al., 1996; Molenaar et al., 1996).

Wnt-stimulated *Cttnb1* gene expression is a post-transcriptionally-regulated mechanism (Gherzi et al., 2006; Bikkavilli and Malbon, 2010). Transcripts of post-transcriptionally regulated genes display AU-rich elements (AREs) in their 3'-untranslated regions (3'-UTRs). AREs act as binding sites for RNA-binding proteins, which either stabilize or destabilize the mRNA transcripts that bind to them. Although only a speculation, it seems likely that RNA-binding proteins might also bind to *Cttnb1* mRNA. Such RNA-binding proteins also display predominant sites of a unique form of post-translational modification: arginine methylation (Bedford and Clarke, 2009; Lee and Stallcup, 2009). Nitrogen atoms of arginine residues within the protein can be post-translationally methylated, catalyzed by a class of enzymes called protein arginine methyl transferases (PRMTs) (Bedford and Richard, 2005; Bedford and Clarke, 2009; Lee and Stallcup, 2009). Previously, we identified a post-transcriptional mechanism of Wnt-dependent regulation of *Cttnb1* mRNA that operated through the Dvl3–KSRP complex (Bikkavilli and Malbon, 2010). As a strategy to more efficiently identify potential RNA-binding proteins involved in the regulation of *Cttnb1* mRNA, we tested for Wnt-stimulated protein arginine methylation events that might reveal novel RNA-binding proteins. Using such a strategy, we identified Ras GTPase activating protein-binding protein 1 (G3BP1). G3BP1 is shown to be a novel Dishevelled-associated protein that is methylated in response to Wnt3a and also binds and regulates *Cttnb1* mRNA. G3BP1 methylation is also shown to constitute a molecular switch that regulates *Cttnb1* mRNA in response to Wnt3a.

Results

G3BP1 is a Dishevelled-associated protein

To identify potential RNA-binding proteins involved in Wnt-dependent regulation of *Cttnb1* mRNA, we searched for Wnt-

dependent methylation products in Dvl3-based supermolecular signaling complexes (Yokoyama et al., 2010). The strategy was to treat totipotent mouse embryonic teratocarcinoma F9 cells with Wnt3a, isolate the Dvl3-based complexes using antibodies against Dvl3, and scan for arginine-methylated proteins. The Dvl3-based pull downs were subjected to SDS-PAGE and the methylated proteins within the signaling complexes were detected by immunoblotting with an antibody that specifically detects mono- and di-methyl arginine (Fig. 1A). With the exception of the light (~20 kDa) and heavy (~50 kDa) chains of IgG that would be expected, only one major methylated protein(s) (~70 kDa) was positively identified (Fig. 1A). Wnt3a, but not Wnt5a (not shown), showed a marked, progressive increase in arginine-methylation of this ~70 kDa protein. The area of the gel of interest was excised and subjected to either trypsin or chymotrypsin digestion. The resulting peptide fragments were analyzed by liquid chromatography and mass spectrometry (LC-MS) using an LTQ ion-trap mass spectrometer equipped with a nano LC electrospray ionization (ESI) source. A methylated peptide was positively identified as that of Ras GTPase activating protein-binding protein 1 (G3BP1, Fig. 1B,C). The ESI mass spectrum of a peptide revealed a doubly charged peak that corresponded to a monomethylated sequence of RGPGGPRGGPSGGMR (amino acids 428–441 of G3BP1). A fragment ion (MS/MS) spectrum further showed that the first arginine (R433 of full-length G3BP1) was monomethylated (Fig. 1B). The primary sequence of G3BP1 encodes an N-terminal Nuclear Transport Factor 2-like domain (NTF2 domain), an RNA recognition motif (RRM domain), and an Arg-Gly-rich region (RGG-rich region, Fig. 1D). The RRM domain and RGG rich regions function canonically in RNA binding of known RNA-binding proteins.

The pull-down data with antibodies against Dvl3 identified G3BP1 as a Dishevelled-associated protein. Ectopic co-expression

of HA-Dvl3 and Myc-G3BP1 in F9 cells was used to further interrogate this association. Immunoprecipitations performed on whole-cell lysates using anti-HA antibodies revealed G3BP1-Dvl3 association (Fig. 2A). We next tested the ability of the N- and C-terminal regions of G3BP1 to associate with Dvl3. HA-tagged Dvl3 was expressed in the absence or presence of Myc-tagged full-length (1–465), N-terminal (1–240) or C-terminal (241–465) G3BP1. Immunoprecipitation of Dvl3 was then performed using anti-HA antibodies. G3BP1 was found to associate with Dvl3-based complexes (Fig. 2B). The C-terminal (241–465) region of G3BP1 similarly associated with Dvl3-based complexes (Fig. 2B). The N-terminal (1–240) region of G3BP1, by contrast, failed to associate with Dvl3-based complexes (Fig. 2B).

We assessed next whether the G3BP1-Dvl3 association was Wnt sensitive. Stimulation of F9 cells overexpressing Myc-tagged G3BP1 with purified Wnt3a revealed a Wnt-dependent dissociation of G3BP1 from the Dvl3-based complexes (Fig. 2C). A transient increase in the amount of G3BP1 associated with the Dvl3-based complex was observed during the first hour of Wnt3a stimulation. Remarkably, following further stimulation with Wnt3a, the amount of G3BP1 associated with the Dvl3-based complex declined (Fig. 2C).

Role of PRMT1 in G3BP1 methylation

Arginine methylation of proteins can be catalyzed by protein arginine methyl transferase 1 (PRMT1), a ubiquitously expressed methyl transferase for histones and other nuclear proteins that bind nucleic acids (Bedford and Clarke, 2009; Lee and Stallcup, 2009). Because G3BP1 was prominently methylated by Wnt3a in the Dvl3-based complex, we evaluated whether PRMT1 was catalyzing the process. Pull-downs performed on F9 cell extracts expressing HA-tagged PRMT1 and Myc-tagged G3BP1 revealed PRMT1-G3BP1 association in these complexes (Fig. 3A). Pull-

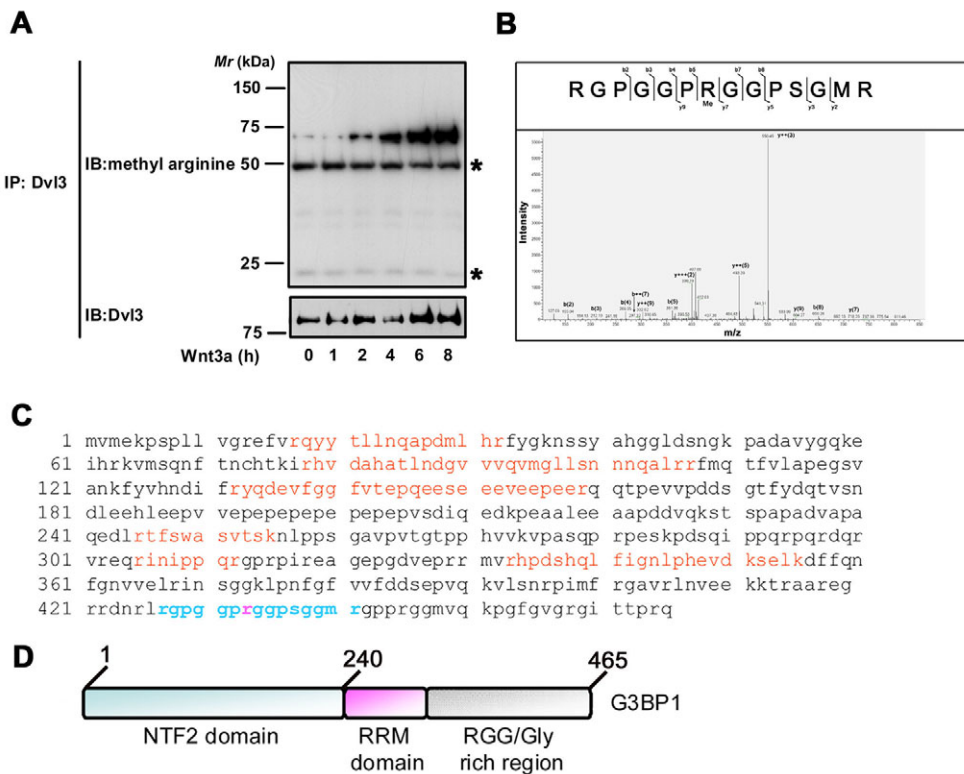


Fig. 1. G3BP1 is a Dishevelled-associated methylated protein. (A) F9 cells were treated with Wnt3a for different durations as indicated, followed by cell lysis and affinity pull-downs with anti-Dvl3 mouse monoclonal antibody. Methylation status of Dvl3-based complexes was then visualized by probing the blots with antibodies that specifically detect either mono or di-methyl arginines on proteins. Strong Wnt-induced methylation of a Dishevelled-associated protein was observed in the molecular range of 50–80 kDa. (B) Fragment ion (MS/MS) spectrum resulting from a doubly charged peptide isolated from the excised band of interest. Monomethylation at R433 of full-length G3BP1 was detected. (C) Primary sequence of mouse G3BP1. Six peptides (Highlighted in red) sequenced from the polypeptides co-purified with Dvl3 matched G3BP1. One peptide (highlighted in blue) was monomethylated. (D) Schematic representation of G3BP1 structure, displaying the NTF2-like domain, an RNA recognition motif and an RG-rich motif.

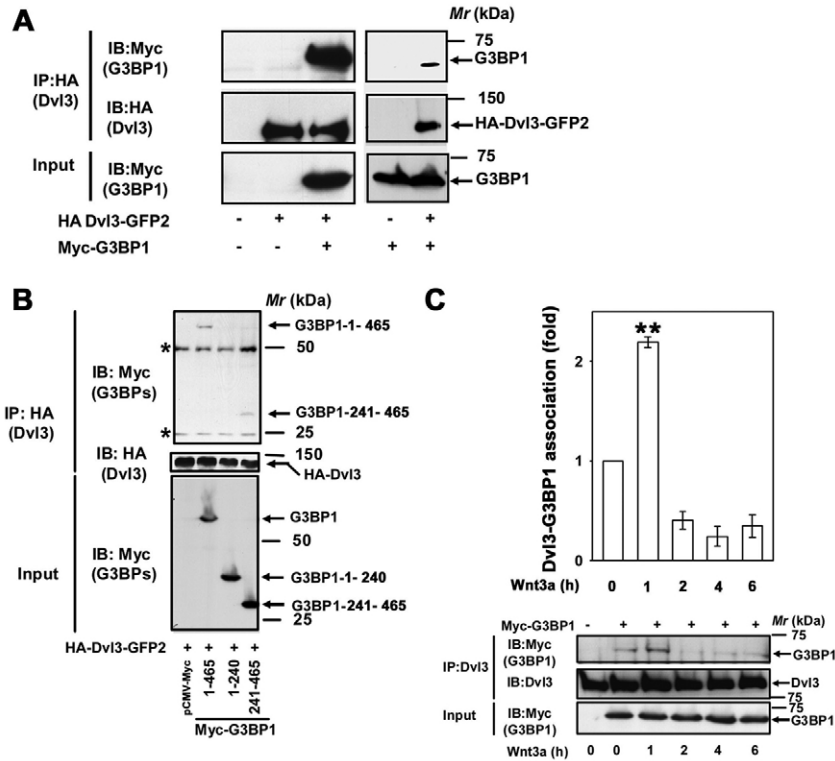


Fig. 2. G3BP1 interacts with Dvl3. (A) F9 cells were transiently transfected with Myc-G3BP1 either alone or with HA-Dvl3-GFP2 for 24 hours followed by cell lysis and affinity pull-downs with anti-HA antibodies. Interaction of G3BP1 with Dvl3 was visualized by probing the blots with anti-Myc antibodies. (B) F9 cells were transfected either with HA-Dvl3-GFP2 alone or with full-length G3BP1 (1–465), its N-terminal half (1–240) or its C-terminal half (241–465) for 24 hours followed by cell lysis and affinity pull-downs with anti-HA antibodies. Interaction of G3BP1 with Dvl3 was visualized by probing the blots with anti-Myc antibodies. (C) F9 cells were transiently transfected with empty vector or Myc-G3BP1 for 24 hours. The cells were then treated with Wnt3a (20 ng/ml) for indicated periods of time followed by cell lysis and affinity pull-downs with anti-Dvl3 specific antibodies followed by immunoblotting with anti-Myc antibodies. Top panel displays mean values \pm s.e.m. obtained from three independent highly reproducible experiments; the lower panel displays representative blots. Asterisks indicate the bands of immunoglobulin heavy and light chains. Representative blots of three independent experiments that proved highly reproducible are displayed. ** $P < 0.01$ versus control (–Wnt3a).

downs with control IgG antibodies or antibodies targeting either Dvl3 or glycogen synthase kinase 3 β (GSK3 β), by contrast, failed to show any association with PRMT1 (Fig. 3A). We probed next whether the PRMT1–G3BP1 association was Wnt sensitive. Stimulation of F9 cells (overexpressing Myc-tagged G3BP1 and HA-tagged PRMT1) with purified Wnt3a provoked a transient increase in the amount of G3BP1 associated with the PRMT1 (Fig. 3B). The Wnt3a-stimulated G3BP1–PRMT1 interaction peaked within 2 hours of treatment. The amount of G3BP1 associated with the PRMT1 declined thereafter (Fig. 3B). We next performed an *in vitro* methylation assay to test directly whether G3BP1 was a PRMT1 substrate. PRMT1 was isolated by immunoprecipitation from F9 cell extracts, whereas recombinant GST–G3BP1 (rG3BP1) was purified in bacteria. The *in vitro* reaction included the isolated PRMT1, purified rG3BP1 and radiolabeled S-adenosyl L-methionine (SAM) as a methyl group donor. PRMT1 isolated from cell extracts of unstimulated cells failed to methylate rG3BP1 (Fig. 3C). Stimulation with Wnt3a, on the contrary, resulted in a marked, progressive PRMT1-catalyzed methylation of G3BP1 (Fig. 3C).

The protein sequence of G3BP1 was scanned for putative PRMT1-methylation motifs. Mass spectrometry has established Arg433 (R433) as one such motif. A second possible methylation motif is R445. To test whether the R433 and R445 were methylated in response to Wnt3a, we made methylation-deficient mutants of G3BP1. Arginine–lysine substitution (both residues are similarly charged) at R433 (R433K) and R445 (R445K) were created in the full-length G3BP1. Upon Wnt3a stimulation, wild-type G3BP1 was efficiently methylated by PRMT1, whereas the R433K mutant was poorly methylated (Fig. 3D). The R445K mutation of G3BP1 did not influence the ability of Wnt3a to stimulate the PRMT1-mediated methylation of G3BP1 (Fig. 3D). Differential activation

of PRMT1 by Wnt3a probably explains the inability of PRMT1 isolated from unstimulated F9 cells to methylate (Fig. 3C) or not (Fig. 3D), GST–G3BP1 under these *in vitro* conditions.

In vivo, we made use of metabolic labeling to discern arginine methylation of G3BP1 and its mutants. F9 cells were transfected to express tagged versions of wild-type G3BP1, as well as the methylation-deficient mutants (R433K and R445K) of G3BP1. Pull-downs from cells expressing wild-type G3BP1 displayed methylation of G3BP1 (Fig. 3E). Pull-downs performed from cells transfected with pCMV–Myc control plasmid served as a negative control for translation cessation (Fig. 3E). Arginine–lysine substitutions at R433 and R445 of G3BP1 severely impacted the *in vivo* methylation status of G3BP1 (Fig. 3E).

G3BP1 negatively regulates Wnt/ β -catenin signaling

To test whether G3BP1 expression modulated canonical Wnt/ β -catenin signaling, Wnt-stimulated β -catenin accumulation and Lef/Tcf-sensitive gene transcription was probed. Knockdown of G3BP1 was effective, in response to treatment with small interfering RNAs (siRNAs). G3BP1 deficiency provoked a twofold increase in basal *Cttnb1* mRNA levels (Fig. 4A). Cells treated with scrambled siRNAs as a control, displayed no such increase (Fig. 4A). G3BP1 deficiency likewise provoked a twofold increase in β -catenin protein levels (Fig. 4B). More telling, G3BP1 deficiency was found to potentiate the ability of Wnt3a to stimulate β -catenin accumulation, the hallmark of canonical Wnt/ β -catenin signaling (Fig. 4B). Knockdown of G3BP1 provoked not only an increase in β -catenin protein, but also a consequential increase in Wnt-stimulated Lef/Tcf-sensitive transcription (Fig. 4C). Overexpression of G3BP1 might be expected to attenuate canonical signaling. Indeed, increased expression of G3BP1 attenuated Wnt3a-stimulated β -catenin levels (Fig. 4D).

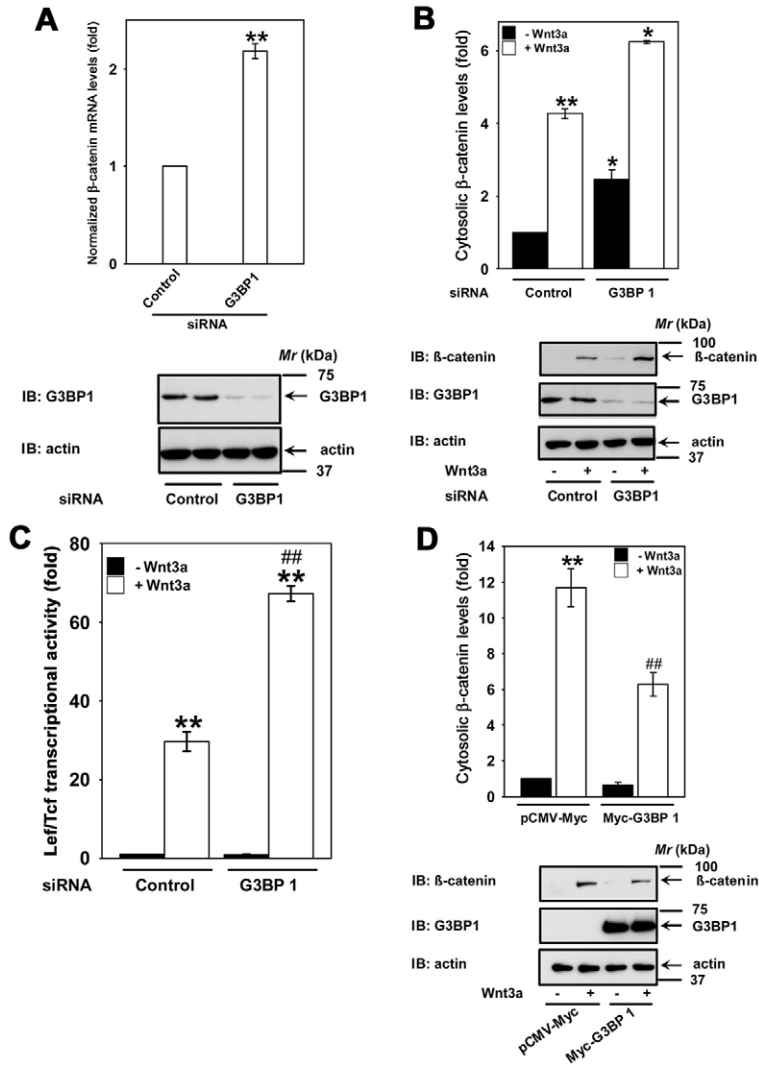


Fig. 4. G3BP1 negatively regulates Wnt/β-catenin signaling. (A) F9 cells were treated with either control siRNAs (100 nM) or siRNAs specific to mouse *G3bp1* (100 nM) for 48 hours and the levels of mRNA encoding β-catenin and cyclophilin A were quantified using quantitative PCR. The data represent normalized *Ctnnb1* mRNA to the *Ppia* (cyclophilin A) mRNA levels (mean values ± s.e.m.) from two independent experiments whose results were in high agreement. ** $P < 0.01$ versus control (control siRNA). F9 cells were treated with either control siRNA (100 nM) or siRNAs specific for mouse *G3bp1* (100 nM) for 48 hours and the lysates were assayed either for cytosolic β-catenin levels (B) or Lef/Tcf-sensitive transcription (C). Top panel displays mean values ± s.e.m. obtained from three independent experiments; the bottom panel displays representative blots. * $P < 0.05$; ** $P < 0.01$ versus unstimulated control (-Wnt3a). ## $P < 0.01$ versus stimulated control (+Wnt3a). (D) F9 cells were transfected with Myc-G3BP1 for 24 hours and the lysates were assayed for cytosolic β-catenin stabilization. Top panel displays mean values ± s.e.m. obtained from three independent experiments; the bottom panel displays representative blots. ** $P < 0.01$ versus unstimulated control (-Wnt3a). ## $P < 0.01$ versus stimulated control (+Wnt3a).

G3BP1 binds *Ctnnb1* mRNA in vivo

G3BP1 is known to bind the 3'-untranslated regions (3'-UTRs) of *Myc* or *Tau* mRNAs (Gallouzi et al., 1998; Liu et al., 1999; Tourriere et al., 2001; Atlas et al., 2004; Atlas et al., 2007). *Ctnnb1* mRNA is present in Dvl3-based complexes (Bikkavilli and Malbon, 2010). Because it has domains necessary for RNA binding, G3BP1 was tested for its ability to bind *Ctnnb1* mRNA. The presence of *Ctnnb1* mRNAs in the G3BP1 complex was probed. *Myc*-G3BP1 and its N-terminal or C-terminal complexes were isolated from cell lysates by immunoprecipitation with anti-Myc antibodies. RNA was isolated from the pull-downs and amplified by RT-PCR. *Ctnnb1* transcripts were found in the G3BP1 complex (Fig. 5A). Pull-downs prepared from lysates of cells transfected with empty pCMV vector, by contrast, displayed no detectable *Ctnnb1* mRNA (Fig. 5A). Pull-downs performed with cells expressing the C-terminal region of G3BP1 (241–465) also displayed *Ctnnb1* transcripts (Fig. 5A). However, pull-downs performed with cells expressing the N-terminal region (1–240 amino acids) of G3BP1, did not display any *Ctnnb1* mRNA (Fig. 5A). Therefore, G3BP1 appears to bind and regulate *Ctnnb1* mRNA.

G3BP1 binds *Ctnnb1* mRNA in vitro

The interaction of G3BP1 and *Ctnnb1* mRNA was investigated in vitro, using northwestern blotting. Probing the blots of recombinant GST or GST-G3BP1 proteins that were transferred onto nitrocellulose membranes by western blotting with an in vitro transcribed digoxigenin (DIG)-labeled full-length *Ctnnb1* UTR (2517–3536) demonstrated binding of the *Ctnnb1* mRNA probe to G3BP1 (Fig. 5B). The *Ctnnb1* mRNA probe also bound G3BP1 immunoprecipitated from cell lysates (Fig. 5C). However, the *Ctnnb1* mRNA probe failed to bind either GST protein (Fig. 5B) or proteins from control (pCMV-Myc empty vector) immunoprecipitations (Fig. 5C). The *Gapdh* mRNA, tested as a control, did not bind G3BP1 (Fig. 5B).

Mapping of the 3'-UTR of *Ctnnb1* mRNA for the binding site of G3BP1

The 3'-UTR of *Ctnnb1* mRNA was probed for the site(s) to which G3BP1 binds. *Ctnnb1* 3'-UTR regions were truncated (2517–2857, 2858–3198, 3199–3536) and DIG-labeled RNA probes of each region were synthesized in vitro using T7 RNA polymerase. The binding of the probes to G3BP1 isolated from cells was then

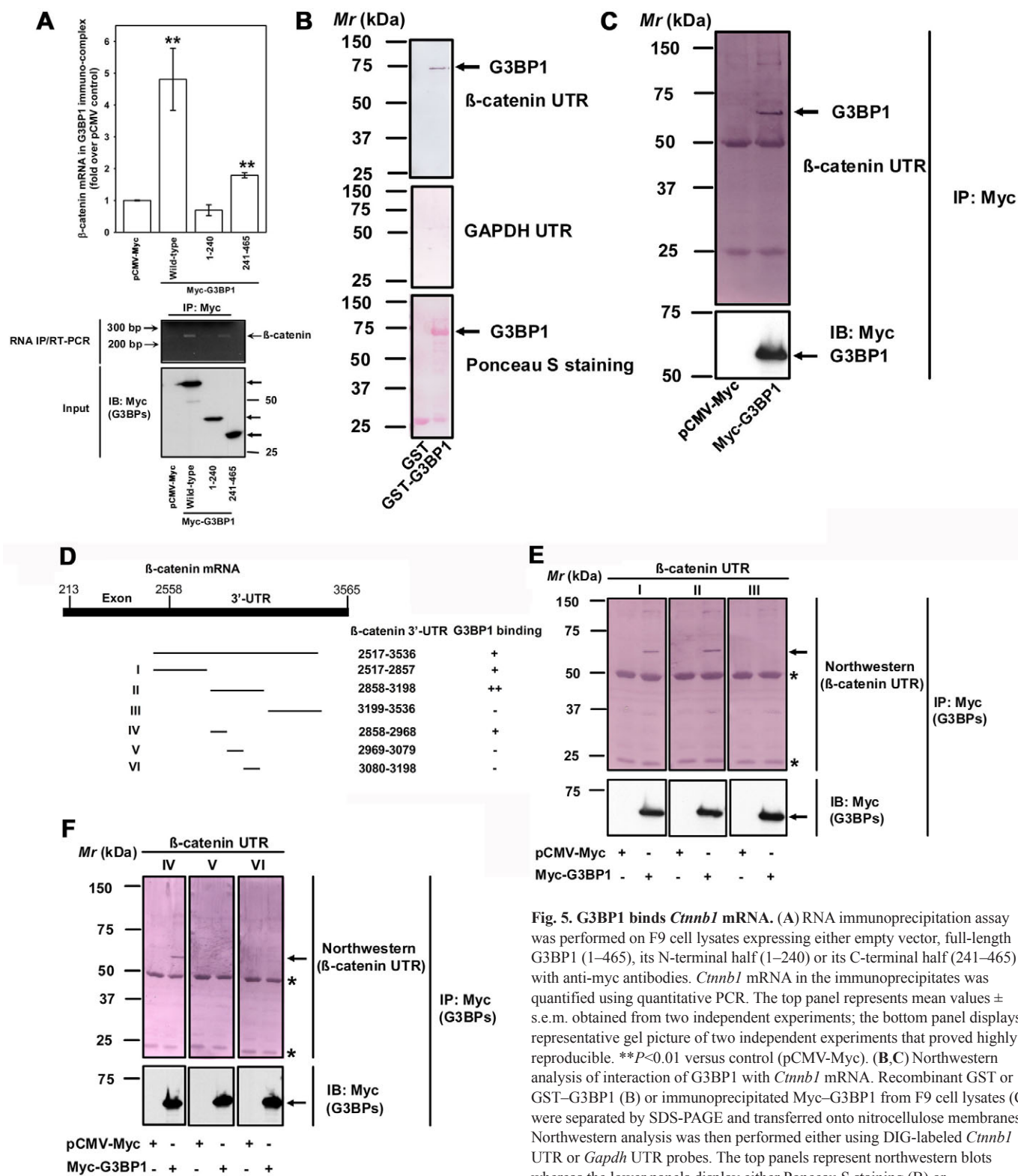


Fig. 5. G3BP1 binds *Cttnb1* mRNA. (A) RNA immunoprecipitation assay was performed on F9 cell lysates expressing either empty vector, full-length G3BP1 (1–465), its N-terminal half (1–240) or its C-terminal half (241–465) with anti-myc antibodies. *Cttnb1* mRNA in the immunoprecipitates was quantified using quantitative PCR. The top panel represents mean values \pm s.e.m. obtained from two independent experiments; the bottom panel displays representative gel picture of two independent experiments that proved highly reproducible. $**P < 0.01$ versus control (pCMV-Myc). (B,C) Northwestern analysis of interaction of G3BP1 with *Cttnb1* mRNA. Recombinant GST or GST–G3BP1 (B) or immunoprecipitated Myc–G3BP1 from F9 cell lysates (C) were separated by SDS-PAGE and transferred onto nitrocellulose membranes. Northwestern analysis was then performed either using DIG-labeled *Cttnb1* UTR or *Gapdh* UTR probes. The top panels represent northwestern blots whereas the lower panels display either Ponceau S staining (B) or immunoblotting with anti-Myc antibodies for the same blots. (D–F) Identification of G3BP1 binding region within the 3'-UTR of *Cttnb1* mRNA. Immunoprecipitated Myc–G3BP1 from F9 cell lysates were separated on SDS-PAGE gels and transferred onto nitrocellulose membranes. Northwestern analysis was then performed using truncated versions of DIG-labeled *Cttnb1* UTR probes. The top panels represent northwestern blots, whereas lower panels display immunoblots with anti-Myc antibodies. Representative data of two independent experiments that proved highly reproducible are displayed.

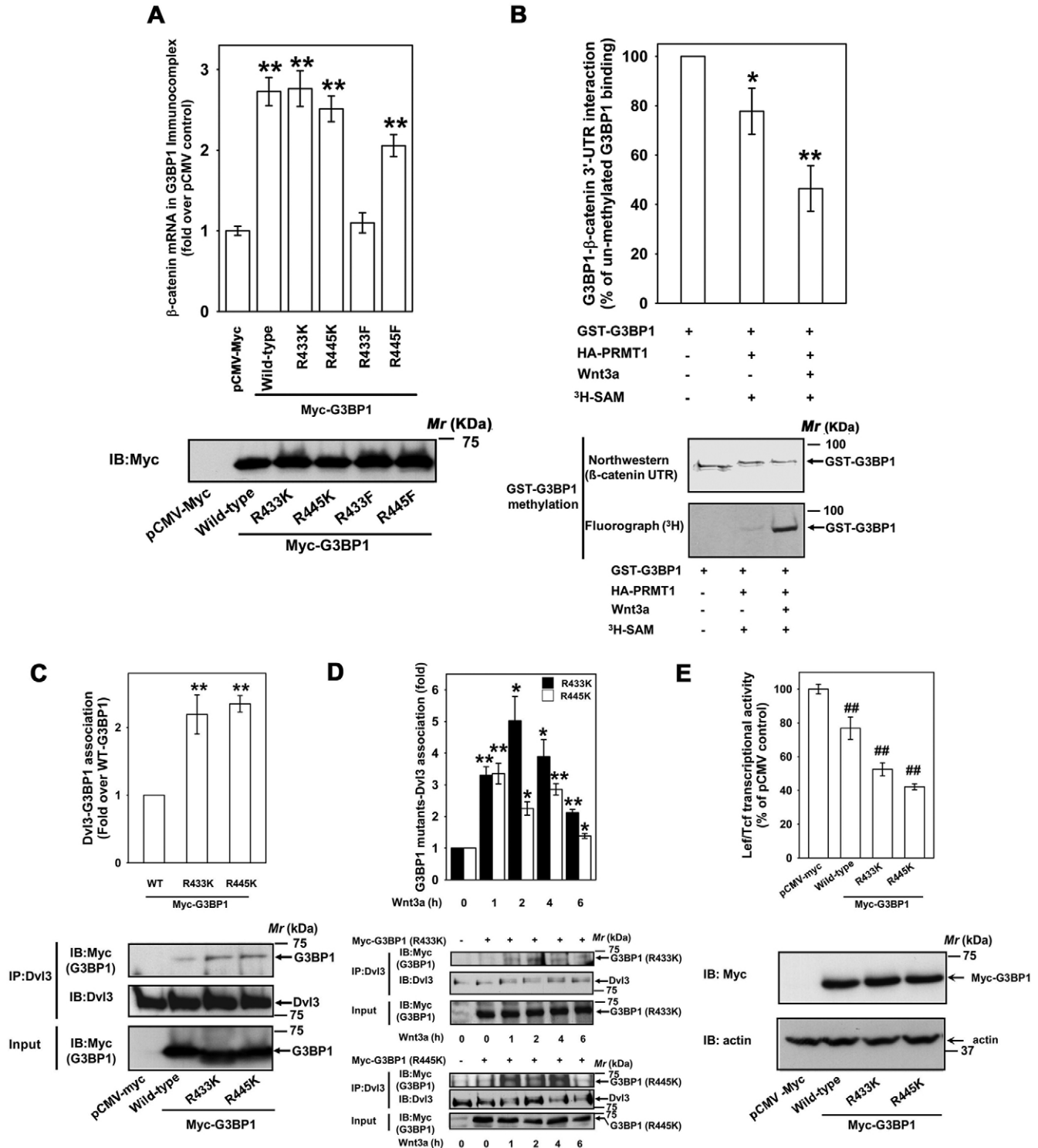


Fig. 6. See next page for legend.

evaluated. RNA probes encoding the 2517–2857 and 2858–3198 regions of *Ctnnb1* UTR bound G3BP1 (Fig. 5E). The 3199–3536 region of *Ctnnb1* UTR, by contrast, failed to bind G3BP1 (Fig. 5E).

G3BP1 has been proposed to be an endoribonuclease selectively cleaving between 'CA' dinucleotides: an activity that requires a binding consensus sequence (Tourriere et al., 2001). Through in

silico searches, we identified a putative G3BP1-binding consensus sequence within the 3'-UTR of *Ctnnb1* mRNA (2885–2907 nucleotides). Therefore, RNA probes encoding additional truncations of the *Ctnnb1* mRNA (2858–2968, 2969–3079, 3080–3198) were synthesized and tested for G3BP1 binding. The RNA probe encoding 2858–2968 region of the *Ctnnb1* mRNA displayed the greatest G3BP1 binding (Fig. 5F). The in silico search also

Fig. 6. Arginine methylation of G3BP1 impairs its binding to *Cttnb1* mRNA and Dvl3. (A) RNA immunoprecipitation assay was performed on F9 cell lysates expressing either empty vector, wild-type G3BP1, its methylation-deficient mutants (R433K, R445K) or its methylation-mimicking mutants (R433F, R445F) with anti-Myc antibodies. The amount of *Cttnb1* mRNA in the immunoprecipitates was then quantified using quantitative PCR. $**P < 0.01$ versus control (pCMV-Myc). (B) Northwestern analysis of unmethylated or methylated GST–G3BP1 and *Cttnb1* mRNA. Equal amounts of unmethylated or methylated (with PRMT1 isolated from unstimulated cells or cells treated with Wnt3a for 6 hours and [3 H]SAM) GST–G3BP1 were separated on SDS-PAGE gels and transferred onto nitrocellulose membranes. Northwestern analysis was then performed on the blots using DIG-labeled *Cttnb1* UTR. The binding of *Cttnb1* mRNA to unmethylated GST–G3BP1 was taken as 100%. The top panel represents mean values \pm s.e.m. obtained from three independent experiments; the bottom panels display northwestern blots and the corresponding fluorograph. $*P < 0.05$; $**P < 0.01$ versus control (unmethylated GST–G3BP1). (C) F9 cells were transiently transfected with either pCMV–Myc, Myc–G3BP1 or its methylation-deficient mutants (R433K, R445K) for 24 hours followed by cell lysis and affinity pull-downs with anti-Dvl3 antibodies. Interaction of G3BP1 and its mutants with Dvl3 was made visible by probing the blots with anti-Myc antibodies. Top panel displays mean values \pm s.e.m. obtained from three independent experiments; bottom panel displays representative blots. $**P < 0.01$ versus control (WT). (D) F9 cells were transiently transfected with methylation-deficient mutants of Myc–G3BP1 (R433K, R445K) for 24 hours. The cells were then treated with Wnt3a (20 ng/ml) for indicated periods of time followed by cell lysis and affinity pull-downs with anti-Dvl3 antibodies followed by immunoblotting with anti-Myc antibodies. Top panel displays mean values \pm s.e.m. obtained from three independent highly reproducible experiments; the bottom panel displays representative blots. $*P < 0.05$; $**P < 0.01$ versus corresponding unstimulated control (–Wnt3a). (E) F9 cells were transfected either with Myc–G3BP1 or its methylation-deficient mutants (R433K, R445K) for 24 hours and the lysates were assayed for *Lef/Tcf*-sensitive transcription following stimulation with Wnt3a for 7 hours. Top panel displays mean values \pm s.e.m. obtained from three independent highly reproducible experiments; bottom panel displays representative blots. $^{##}P < 0.01$ versus control (pCMV-Myc).

identified this region (2885–2907) of *Cttnb1* mRNA for G3BP1 binding. The two other RNA probes tested did not bind G3BP1 (2969–3079 and 3080–3198, Fig. 5F).

Arginine methylation of G3BP1 is a molecular switch, provoking dissociation from *Cttnb1* mRNA and Dishevelled-based supermolecular complexes

Does methylation of G3BP1 alter its binding of *Cttnb1* mRNA? Myc-tagged wild-type G3BP1 and methylation-deficient (R433K, R445K) and methylation-mimicking [R433F, R445F (Mostaouf et al., 2006; Weber et al., 2009; Guo et al., 2010)] mutants of G3BP1 were used to address this question. Cells were transiently transfected with either wild-type or mutant forms of G3BP1 and cell lysates were later subjected to pull-downs with anti-Myc antibodies. Isolation of RNA (from Myc pull-downs) and amplification by RT-PCR was performed next. The relative amounts of *Cttnb1* transcripts in the G3BP1 complexes were then established using quantitative real-time PCR. *Cttnb1* transcripts were identified in the wild-type G3BP1 pull-downs (Fig. 6A). By contrast, *Cttnb1* transcripts were nearly undetectable in the pull-downs from cells expressing R433F mutant of G3BP1 (a ‘methylation-mimicking mutant’, Fig. 6A). Binding of *Cttnb1* mRNA to G3BP1 was unaffected by the R445F mutation, being similar to either wild-type or methylation-deficient mutants (R433K, R445K, Fig. 6A). To further test the role of arginine methylation in the association of G3BP1 with *Cttnb1* mRNA, we examined whether methylation of GST–G3BP1 affects its ability

to bind *Cttnb1* mRNA in vitro. For these experiments, methylated GST–G3BP1 was prepared in vitro using HA–PRMT1. Methylation was assessed through the use of tritiated-S-adenosyl methionine ([3 H]SAM) in the methylation assay buffer. Equal amounts of unmethylated and methylated GST–G3BP1 were separated on SDS-PAGE gels and transferred to nitrocellulose membranes. Northwestern analysis was then performed on the membranes using a DIG-labeled full-length *Cttnb1* UTR. Consistent with the RNA immunoprecipitation data (Fig. 6A), Wnt3a-stimulated PRMT1-mediated methylation of GST–G3BP1 provoked a sharp decrease in the ability of G3BP1 to bind *Cttnb1* mRNA (Fig. 6B). Methylation of GST–G3BP1 by PRMT1 isolated from untreated cells provoked a small decrease in the ability of G3BP1 to bind *Cttnb1* mRNA (Fig. 6B). Arginine methylation of G3BP1 appears to be a molecular switch: in response to methylation at R433, the ability of G3BP1 to bind *Cttnb1* mRNA was sharply attenuated (Fig. 6A,B).

G3BP1 is a Dishevelled-associated protein (Fig. 2) that is methylated upon Wnt3a stimulation (Fig. 3). We assessed whether G3BP1 methylation influences its ability to bind Dvl3. F9 cells overexpressing either Myc-tagged wild-type G3BP1 or methylation-deficient mutants (R433K and R445K) of G3BP1 were used to address this question. Pull-downs performed on cell lysates using anti-Dvl3 antibodies show greater association of the methylation-deficient mutants (R433K and R445K) of G3BP1 than wild-type G3BP1 to Dvl3 (Fig. 6C). Wnt3a stimulation of cells that overexpress wild-type G3BP1 provoked loss of G3BP1 from the Dvl3-based supermolecular complex (Fig. 2). Wnt3a stimulation of cells overexpressing methylation-deficient mutants (R433K and R445K), by contrast, did not release G3BP1 from the Dvl3-based supermolecular complex (Fig. 6D). These observations suggest that arginine methylation of G3BP1 provokes the release of G3BP1 from the Dvl3-based signaling complex.

Would expression of methylation-deficient (R433K and R445K) mutants of G3BP1 alter canonical Wnt/ β -catenin signaling? *Lef/Tcf*-sensitive gene transcription was assessed in cells expressing R433K or R445K G3BP1. Overexpression of wild-type G3BP1 decreased Wnt3a-stimulated *Lef/Tcf*-sensitive transcription (Fig. 6E). However, expression of the methylation-deficient mutants of G3BP1 attenuated the Wnt3a-stimulated *Lef/Tcf*-sensitive transcription further (Fig. 6E). In tandem, these observations make a compelling case for protein methylation as the regulator for G3BP1 binding of *Cttnb1* mRNA, as well as its docking to Dvl3-based signalsomes that catalyze canonical signaling.

Discussion

Dishevelled is a multi-functional scaffold protein that has a critical role(s) during Wnt signaling. Dishevelled, through its common domains such as DIX, PDZ and DEP domains, provides docking sites for many proteins and constitutes a large supermolecular assembly (Yokoyama et al., 2010). In the present study, G3BP1 was identified as a novel Dishevelled-associated protein. G3BP1 associates with Dishevelled through its C-terminus, which displays arginine methylation (RGG) motifs. Wnt3a stimulated robust methylation of G3BP1. Methylation of G3BP1 also provoked reduced association with the Dishevelled-based complexes.

G3BP1 was discovered as a Ras GTPase activating (Ras GAP) SH3-binding protein (Parker et al., 1996). The critical role of G3BPs during mammalian and invertebrate development is highlighted in several studies using either knockout mice (Zekri et

al., 2005) or zebrafish (Irvine et al., 2004). G3BPs are also known to have important roles in Ras biology (Parker et al., 1996) and ubiquitin signaling (Soncini et al., 2001). The primary sequence of G3BP1 displays RNA recognition and arginine methylation motifs canonically associated with RNA binding. G3BP1 is known also to regulate transcripts of *Myc*, *Tau* and β -F1ATPase (Tourriere et al., 2001; Atlas et al., 2007; Ortega et al., 2010). In the present study, we show that G3BP1 binds *Ctnnb1* mRNA. Depletion of G3BP1 also resulted in the upregulation of *Ctnnb1* mRNA and β -catenin protein levels (Fig. 4). Therefore, G3BP1 appears to dock *Ctnnb1* mRNA (at the consensus binding site, 2885–2907), subjecting *Ctnnb1* mRNA to degradation. This mechanism would be similar to that reported for G3BP1-mediated regulation of *Myc* mRNA (Tourriere et al., 2001).

Direct evidence is provided also for Wnt3a-stimulated G3BP1 methylation by PRMT1. Wnt stimulation triggers PRMT1-mediated methylation of the wild type and the R445K mutant of G3BP1, but not the R433K mutant. Strikingly, the R433F (methylation-mimicking) mutation of G3BP1 provokes a complete loss of *Ctnnb1* mRNA binding ability. These observations strongly suggest that methylation of G3BP1 at R433 by PRMT1 constitutes a key regulatory step in canonical Wnt/ β -catenin signaling.

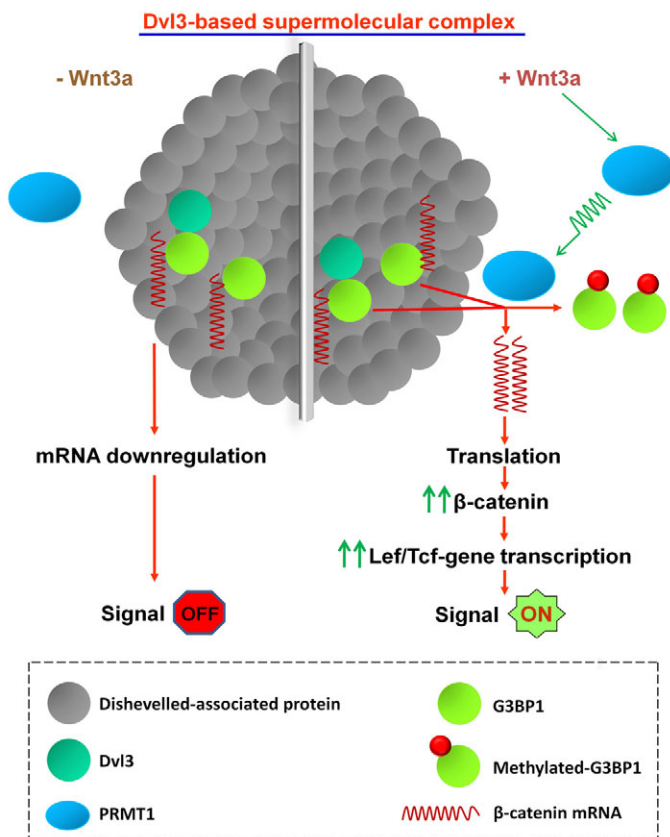


Fig. 7. Arginine methylation of G3BP1 regulates both *Ctnnb1* mRNA and canonical Wnt/ β -catenin signaling. In the absence of Wnt stimulation (–Wnt3a), the G3BP1 of Dvl3-based supermolecular complex (signalsomes) binds and regulates *Ctnnb1* mRNA (left). Stimulation of cells by Wnt3a activates PRMT1, which methylates G3BP1, provoking release of *Ctnnb1* mRNA as well as release of G3BP1 from the signalsome. Increased *Ctnnb1* mRNA provokes increased accumulation of β -catenin and activation of canonical Wnt pathway via Lef/Tcf-sensitive gene transcription.

We show herein a previously unidentified role for protein arginine methylation in canonical Wnt/ β -catenin signaling, focusing upon *Ctnnb1* mRNA. *Ctnnb1* mRNA is regulated post-transcriptionally (Gherzi et al., 2006; Bikkavilli and Malbon, 2010). Now we show a post-translational modification-mediated regulation of *Ctnnb1* mRNA. Under basal conditions, the Dvl3–G3BP1 complex actively mediates downregulation of *Ctnnb1* mRNA. Wnt3a stimulation provokes methylation of G3BP1 by PRMT1, releasing *Ctnnb1* mRNA from this regulatory degradation. We propose that protein arginine methylation is a Wnt3a-sensitive ‘molecular switch’ that fosters decreased binding of *Ctnnb1* mRNA to G3BP1, which accompanies loss of G3BP1 from the Dvl3-based signalsome (Fig. 7). The molecular details of these altered interactions of G3BP1 and *Ctnnb1* mRNA remain to be discerned; however, their functional role on canonical Wnt signaling is clearly important.

Materials and Methods

Constructs

Mouse Dvl2 and Dvl3 isoforms were engineered in-house with GFP2 and HA tags. cDNAs of *G3bp1* and its fragments (1–240 and 241–465) were subcloned into the *EcoRI* and *NotI* sites of pCMV-Myc plasmid in-frame with the Myc tag sequence. Mouse *Prmt1* cDNA was subcloned into *EcoRI* and *KpnI* sites of pCMV-HA vector in-frame with the HA tag sequence. DNA fragments of mouse *Ctnnb1* 3′-UTR (NM_007614, 2517–3536, 2517–2857, 2858–3198, 3199–3536, 2858–2968, 2969–3079, 3080–3198), and mouse *Gapdh* 3′-UTR (NM_008084, 1011–1230) were subcloned into *KpnI* and *EcoRI* sites of pcDNA3.1 vector. Site-directed mutagenesis was performed on Myc–G3BP1 plasmid using Quick Change Site Directed Mutagenesis kit (Stratagene) to obtain Myc–G3BP1 mutants (R433K, R445K, R433F and R445F). For generating GST-tagged G3BP1, cDNAs encoding G3BP1 and its mutants were subcloned into *EcoRI* and *NotI* sites of pGEX4T1 plasmid in-frame with the GST protein. The primers used for cloning are summarized in supplementary material Table S1.

Cell culture

Mouse F9 teratocarcinoma cell stocks were obtained from ATCC (Manassas, VA) and were maintained in Dulbecco’s modified Eagle’s medium (DMEM) supplemented with 15% (F9 cells) heat-inactivated fetal bovine serum (Hyclone, South Logan, UT) at 37°C in a 5% CO₂ incubator. The F9 cells stably expressing Rfz1 and pTOPFLASH (M50) luciferase reporter were generated as described earlier (Bikkavilli et al., 2008) and used as a standard in all experiments. The use of this stable cell line as the starting point for transient transfections reduced variability and offered greater consistency by reducing the number of plasmids required for simultaneous transfections.

Coimmunoprecipitation and immunoblotting

For coimmunoprecipitation experiments, F9 clones stably expressing rat Frizzled1 were transiently transfected for 24 hours with 6 μ g of plasmid vectors in 100 mm culture dishes. After 24 hours, the cells were lysed in 1 ml of lysis buffer (1 \times PBS, 1% Nonidet P-40, 0.5% sodium deoxycholate, 0.1% SDS, 1 μ g/ml leupeptin, 1 μ g/ml aprotinin and 1 μ g/ml phenylmethylsulphonyl fluoride). The lysates were cleared by centrifugation at 20,000 *g* for 15 minutes, twice. The supernatants were transferred into new tubes and protein concentrations were determined by the Lowry method (Lowry et al., 1951). Immunoprecipitations were performed using either rat anti-HA high affinity (Roche), mouse monoclonal anti-Dvl3 (sc 8027, Santa Cruz), mouse monoclonal anti-Myc antibodies (M4439, Sigma), or mouse anti-GSK3 β (610201, BD Transduction Laboratories) and Protein-A–Sepharose CL-4B (17-0780-01, GE Life Sciences). For immunoblotting, total lysates (30–60 μ g of protein/lane) were subjected to electrophoresis using 10% SDS-PAGE. The resolved proteins were transferred electrophoretically to nitrocellulose membrane ‘blots’. The blots were incubated with primary antibodies overnight at 4°C and immunocomplexes were made visible with a secondary antibody coupled to horseradish peroxidase and developed using the enhanced chemiluminescence method. Antibodies were purchased from the following sources: anti-HA high affinity antibody (Roche Applied Science, Indianapolis, IN), anti- β -catenin, anti-Myc, and anti- β -actin antibodies were from Sigma. Mouse anti-GSK3 β was from BD Transduction Laboratories. Mouse monoclonal anti-monomethyl and anti-dimethyl arginine was from Abcam (ab412).

In-gel tryptic digestion and mass spectrometry analysis

Following SDS-PAGE analysis of Dvl3 immunocomplexes, the gel band corresponding to the molecular range of 50–80 kDa was excised, destained, reduced, alkylated and digested with either trypsin or chymotrypsin (Promega Gold, Mass Spectrometry Grade) essentially as described previously (Shevchenko et al., 1996) with minor modifications. The resulting concentrated peptide extract was diluted

into a solution of 2% acetonitrile (ACN), 0.1% formic acid (FA) (Buffer A) for analysis. 10 μ l of the peptide mixture was analyzed by automated microcapillary liquid chromatography tandem mass spectrometry. Fused-silica capillaries (100 μ m i.d.) were pulled using a P-2000 CO₂ laser puller (Sutter Instruments, Novato, CA) to a 5 μ m i.d. tip and packed with 10 cm of 5 μ m Magic C18 material (Agilent, Santa Clara, CA) using a pressure bomb. This column was then placed in-line with a Dionex 3000 HPLC equipped with an autosampler. The column was equilibrated in buffer A, and the peptide mixture was loaded onto the column using the autosampler. The HPLC separation at a flow rate of 300 nl/minute was provided by a gradient between Buffer A and Buffer B (98% acetonitrile, 0.1% formic acid). The HPLC gradient was held constant at 100% buffer A for 5 minutes after peptide loading followed by a 30 minute gradient from 5% buffer B to 40% buffer B. Then, the gradient was switched from 40% to 80% buffer B over 5 minutes and held constant for 3 minutes. Finally, the gradient was changed from 80% buffer B to 100% buffer A over 1 minute, and then held constant at 100% buffer A for 15 more minutes. The application of a 1.8 kV distal voltage electrosprayed the eluted peptides directly into a Thermo LTQ ion trap mass spectrometer equipped with a custom nanoLC electrospray ionization source. Full mass (MS) spectra were recorded on the peptides over a 400–2000 m/z range, followed by five tandem mass (MS/MS) events sequentially generated in a data-dependent manner on the first, second, third, fourth and fifth most intense ions selected from the full MS spectrum (at 35% collision energy). Mass spectrometer scan functions and HPLC solvent gradients were controlled by the Xcalibur data system (ThermoFinnigan, San Jose, CA). MS/MS spectra were extracted from the RAW file with ReAdW.exe (Sourceforge). The resulting mz XML file contains all the data for all MS/MS spectra and can be read by the subsequent analysis software. The MS/MS data was searched with Inspect (Tanner et al., 2005) against a mouse database (PI v.3.43) plus common contaminants, with modifications: +16 on Met, +57 on Cys, +14 on Arg and Lys. Only peptides with a *P* value of at least 0.02 were analyzed further. Peptides with possible methylated arginines and lysines were manually verified.

In vitro methylation assays

In vitro methylation assay using bacterially expressed GST–G3BP1 was performed as described earlier (Tini et al., 2009). Briefly, F9 cells were transiently transfected with HA–PRMT1 (6 μ g) in 100 mm culture dishes. After 24 hours of transfection, the cells were lysed in a lysis buffer (1 \times PBS, 1% Nonidet P-40, 0.5% sodium deoxycholate, 0.1% SDS, 1 μ g/ml leupeptin, 1 μ g/ml aprotinin and 1 μ g/ml phenylmethylsulphonyl fluoride) after treatment either with or without Wnt3a for different lengths of time. The lysates were then used to immunoprecipitate PRMT1 using anti-HA antibodies and Protein–A–Sepharose CL-4B (17-0780-01, GE Life Sciences) at 4°C for 16 hours. After 16 hours, the immunoprecipitates were washed three times in RIPA buffer (20 mM Tris–HCl, pH 8.0, 150 mM NaCl, 5 mM EDTA and 1% Triton X-100) and once in methylation buffer (50 mM Tris–HCl, pH 8.5, 20 mM KCl, 10 mM MgCl₂, 1 mM β -mercaptoethanol, 100 mM sucrose). Finally, the HA–Sepharose containing bound PRMT1 was incubated with 10 μ l of methylation reaction buffer containing 4 μ g of GST–G3BP1 or its mutants and 1 μ Ci S-adenosyl-L-[methyl-³H] methionine (NEN Radiochemicals, 250 μ Ci, 9.25 MBq), at 30°C for 1 hour. After 1 hour, the reactions were stopped by addition of equal volume of SDS sample loading buffer, boiled and separated on a SDS–PAGE gel. The gel was then fixed (45% methanol, 10% acetic acid in water, 30 minutes), amplified (Autofluor, National Diagnostics, 2 hours), dried and fluorography was performed.

In vivo methylation assays

In vivo methylation assay for G3BP1 was performed as described previously (Tini et al., 2009). Briefly, F9 cells were transiently transfected with pCMV–Myc, Myc–G3BP1 or its mutants (R433K, R445K) (6 μ g) in 100 mm culture dishes and grown to confluency (24 hours). After 24 hours of transfection, the cells were washed once with PBS and protein translation was inhibited by incubating with 100 μ g/ml cycloheximide and 40 μ g/ml chloramphenicol in DMEM medium with 10% FBS for 30 minutes at 37°C. After 30 minutes, the cells were washed once with methionine-free DMEM. Cell-labeling mixture consisting of methionine-free DMEM supplemented with 100 μ g/ml cycloheximide and 40 μ g/ml chloramphenicol and 60 μ Ci L-[methyl-³H]methionine was added to the cells and incubated at 37°C for 3 hours. After 3 hours of metabolic labeling, the cells were lysed in a lysis buffer (1 \times PBS, 1% Nonidet P-40, 0.5% sodium deoxycholate, 0.1% SDS, 1 μ g/ml leupeptin, 1 μ g/ml aprotinin and 1 μ g/ml phenylmethylsulphonyl fluoride). The lysates were then utilized for immunoprecipitations using anti-myc antibodies and Protein–A–Sepharose CL-4B (17-0780-01, GE Life Sciences) for 16 hours at 4°C. After 16 hours, the immunoprecipitates were washed three times in RIPA buffer (20 mM Tris–HCl, pH 8.0, 150 mM NaCl, 5 mM EDTA and 1% Triton X-100) and the beads were resuspended in SDS sample loading buffer, boiled and separated by SDS–PAGE. The gel was then transferred to a nitrocellulose membrane, amplified (Autofluor, National Diagnostics, 2 hours) and fluorography was performed.

Northwestern analysis

Digoxigenin (DIG)-labeled 3'-UTR probes of *Ctnnb1* and *Gapdh* were synthesized in vitro using T7 RNA polymerase (Roche Applied Science) as per the manufacturer's recommendations in the presence of rNTPs and DIG-UTP and

pCDNA3.1 vectors harboring *Ctnnb1* or *Gapdh* UTRs as templates. For northwestern analysis, proteins (recombinant or immunoprecipitated) were resolved by SDS–PAGE and electrophoretically transferred to nitrocellulose membrane blots. The blots were blocked in Tris-buffered saline (TBST, 50 mM Tris–HCl, pH 7.4, 150 mM NaCl and 0.1% Tween 20) containing 5% non-fat milk at 4°C overnight with gentle rocking. DIG-labeled probes (1 μ g/ml in TBST buffer with milk) were added to the blots and incubated at room temperature with gentle rocking for 2 hours. After 2 hours, the blots were washed three times in TBST at 5 minute intervals. The binding of RNA probes to G3BP1 was then revealed by probing the blots with anti-DIG AP fragments diluted (1:1000) in TBST with 5% milk (11093274910, Roche), followed by colorimetric detection of alkaline phosphatase using Nitro-Blue Tetrazolium chloride (NBT) and 5-Bromo-4-Chloro-3'-Indolylphosphate p-Toluidine Salt (BCIP) substrates according to the manufacturer's recommendation (DIG-RNA detection kit, Roche).

Immunoprecipitation of ribonucleoprotein complexes

Ribonucleoprotein complexes were immunoprecipitated from F9 cells transiently expressing pCMV–Myc control, Myc–G3BP1 or its N-terminal (1–240) or C-terminal (241–465) regions or its mutants (R433K, R445K, R433F, R445F) using mouse monoclonal anti-Myc antibodies (9E10, Sigma). Briefly, 6 mg of lysates were incubated with 2.5 μ g anti-Myc antibodies (M4439, Sigma) at 4°C with gentle rotation. After 16 hours, 20 μ l of Protein–A–Sepharose CL-4B (17-0780-01, GE Life Sciences) was added to each tube and incubated at 4°C for 4 hours with gentle rotation. After 4 hours, the resin beads were washed with RIPA buffer (20 mM Tris–HCl, pH 8.0, 150 mM NaCl, 5 mM EDTA and 1% Triton X-100) three times. Total RNA from the immunocomplexes were then isolated using RNA STAT 60 reagent (Tel-test, Friendswood, TX) according to the manufacturer's instructions. After determining the RNA concentrations using a spectrophotometer, first-strand cDNA synthesis was performed using 0.5 μ g of total RNA and Superscript II reverse transcriptase (Invitrogen) and oligo dT(18) primer. Real-time quantitative PCR amplification was performed using the DNA engine Opticon continuous fluorescence detection system (MJ Research, Boston, MA). For a 20 μ l PCR, 8 μ l of cDNA template (previously diluted to 1:15 with water) was mixed with 6.25 pmol of forward and reverse primers and 2 \times SYBR green PCR master mix (Qiagen, Valencia, CA). The Light Cycler was programmed such that it included an initial activation step of 95°C for 15 minutes followed by 40 cycles of denaturation at 95°C for 30 seconds, annealing at 60°C for 30 seconds and extension at 72°C for 1 minute. Each cDNA sample was analyzed in triplicate and the absolute amount of β -catenin template in the immunocomplexes was determined using an external standard. Briefly, a standard curve was generated using cycle threshold (*C_t*) values obtained from real-time PCR using Dvl2 specific primers (supplementary material Table S1) and pGFP2-N2-mDvl2 plasmid (1, 0.1, 0.01 and 0.001 ng/reaction). The *C_t* values of real-time PCR for cDNA from each RNA sample was then substituted in the equation generated from the corresponding standard curve to calculate the amount of the amplicon. The calculated amounts of amplicons (pg) or the fold increase over control values are represented in the graphs.

Cytosolic β -catenin accumulation assay

To separate the cytosolic β -catenin from membrane-associated β -catenin, lysates were treated with Concanavalin–A–Sepharose (ConA, Amersham Biosciences, Uppsala, Sweden), as described previously (Aghib and McCrear, 1995). Briefly, confluent F9 cultures were treated with Wnt3a for 4 hours (Fig. 3B,E,F) and lysed in a lysis buffer (20 mM Tris–HCl, pH 7.4, 150 mM NaCl, 5 mM EDTA, 50 mM NaF, 40 mM Na₂P₂O₇, 50 mM K₂HPO₄, 10 mM Na₂MoO₄, 2 mM Na₃VO₄, 1% Triton X-100, 0.5% NP40, 1 μ g/ml leupeptin, 1 μ g/ml aprotinin and 1 μ g/ml phenylmethylsulphonyl fluoride). The lysates were transferred into 1.5 ml Eppendorf tubes and rotated at 4°C for 15 minutes followed by centrifugation at 20,000 *g* for 15 minutes. The supernatants were transferred into new tubes, their protein concentrations were determined and the concentration was adjusted to 2.5 mg/ml with lysis buffer. 60 μ l of ConA–Sepharose was added to each tube and rotated at 4°C for 1 hour. After a brief centrifugation, the supernatants were transferred to new tubes and 30 μ l of ConA–Sepharose was added to each tube and rotated at 4°C for another hour. Finally, after a brief centrifugation, the supernatants were transferred to new tubes and their protein concentration was determined. Immunoblotting was performed with the samples and β -catenin accumulation was analyzed by probing the blots with anti- β -catenin antibodies and normalized by probing the same blots with anti-actin antibodies.

RNAi

Double-stranded RNAs (siRNAs) targeting mouse *G3bp1* (5'-CCAAGAUGAGGU-CUUCGUGGCUUU-3') and control siRNAs (5'-UCUGUGAAUUGAAA-GACUAGCCAAG-3') were procured from Invitrogen (Invitrogen, Carlsbad, CA). F9 cells expressing Rfz1 were treated with 100 nM siRNA using Lipofectamine 2000 reagent (Invitrogen) according to the manufacturer's protocol. Briefly, 100 nM siRNA was incubated with 5 μ l Lipofectamine 2000 for 20 minutes in 200 μ l Optimem medium (Invitrogen), and the mixture was then added to 1 ml of growth medium in a 12-well plate in which F9 cells expressing Rfz1 were cultured to 80% confluency. After siRNA treatment for 48 hours, the cells were assayed for *Ctnnb1* mRNA levels, β -catenin stabilization or Lef/Tcf-sensitive gene transcription.

Luciferase assays

F9 cells stably expressing Rfz1 and super 8xTOPFLASH (M50) luciferase reporter were seeded into 12-well plates. Following incubation with siRNAs for 48 hours at 37°C, the cells were treated with or without recombinant Wnt3a for 7 hours (R&D systems, Minneapolis). Cells were then directly lysed on the plates by addition of 1× cell culture lysis reagent (Promega, Madison, WI). Lysates were collected into chilled microfuge tubes on ice and centrifuged at 20,000 g for 5 minutes. The supernatant was transferred into a new tube and directly assayed as described below. 20 µl of the lysate was mixed with 100 µl of luciferase assay buffer (20 mM Tricine, pH 7.8, 1.1 mM MgCO₃, 4 mM MgSO₄, 0.1 mM EDTA, 0.27 mM coenzyme A, 0.67 mM luciferin, 33 mM DTT and 0.6 mM ATP) and the luciferase activities were measured with a luminometer (Berthold Lumat LB 9507). The samples were assayed in triplicate and the luciferase activities were normalized by protein content of the samples and are represented in the figures.

Data analysis

Typically, data were compiled from at least three independent replicate experiments, each performed on separate cultures and on separate occasions. We calculated and display the responses as 'fold change' (over the untreated control). Comparisons of data among such groups were performed using the Student's *t*-test for assessing variance. Statistical significance ($P < 0.05$) is denoted with either an asterisk or a pound symbol. For a few of the experiments replicated independently with very low variance, duplicates were deemed adequate. Each of these instances are indicated in their respective figure legends.

We thank Antonius Koller (Technical Director, Proteomics Center, SUNY, Stony Brook) for his help with sample preparation and generation and analysis of MS/MS spectra. We would like to thank Hsien-Yu Wang (Department of Physiology & Biophysics, SUNY, Stony Brook) for critical reading of the manuscript. We thank members of the Malbon and Wang laboratories for their technical advice. This work was supported by USPHS Grant DK30111 from the NIDDK, National Institutes of Health (to C.C.M.). Deposited in PMC for immediate release.

Supplementary material available online at

<http://jcs.biologists.org/cgi/content/full/124/13/2310/DC1>

References

- Aghib, D. F. and McCrea, P. D. (1995). The E-cadherin complex contains the src substrate p120. *Exp. Cell Res.* **218**, 359-369.
- Angers, S. and Moon, R. T. (2009). Proximal events in Wnt signal transduction. *Nat. Rev. Mol. Cell Biol.* **10**, 468-477.
- Atlas, R., Behar, L., Elliott, E. and Ginzburg, I. (2004). The insulin-like growth factor mRNA binding-protein IMP-1 and the Ras-regulatory protein G3BP associate with tau mRNA and HuD protein in differentiated P19 neuronal cells. *J. Neurochem.* **89**, 613-626.
- Atlas, R., Behar, L., Sapoznik, S. and Ginzburg, I. (2007). Dynamic association with polysomes during P19 neuronal differentiation and an untranslated-region-dependent translation regulation of the tau mRNA by the tau mRNA-associated proteins IMP1, HuD, and G3BP1. *J. Neurosci. Res.* **85**, 173-183.
- Bedford, M. T. and Clarke, S. G. (2009). Protein arginine methylation in mammals: who, what, and why. *Mol. Cell* **33**, 1-13.
- Bedford, M. T. and Richard, S. (2005). Arginine methylation an emerging regulator of protein function. *Mol. Cell* **18**, 263-272.
- Behrens, J., von Kries, J. P., Kuhl, M., Bruhn, L., Wedlich, D., Grosschedl, R. and Birchmeier, W. (1996). Functional interaction of beta-catenin with the transcription factor LEF-1. *Nature* **382**, 638-642.
- Bhanot, P., Brink, M., Samos, C. H., Hsieh, J. C., Wang, Y., Macke, J. P., Andrew, D., Nathans, J. and Nusse, R. (1996). A new member of the frizzled family from *Drosophila* functions as a Wingless receptor. *Nature* **382**, 225-230.
- Bikkavilli, R. K. and Malbon, C. C. (2010). Dishevelled-KSRP complex regulates Wnt signaling through post-transcriptional stabilization of beta-catenin mRNA. *J. Cell Sci.* **123**, 1352-1362.
- Bikkavilli, R. K., Feigin, M. E. and Malbon, C. C. (2008). G alpha o mediates WNT-JNK signaling through dishevelled 1 and 3, RhoA family members, and MEKK 1 and 4 in mammalian cells. *J. Cell Sci.* **121**, 234-245.
- Gallouzi, I. E., Parker, F., Chebli, K., Maurier, F., Labourier, E., Barlat, I., Capony, J. P., Tocque, B. and Tazi, J. (1998). A novel phosphorylation-dependent RNase activity of GAP-SH3 binding protein: a potential link between signal transduction and RNA stability. *Mol. Cell Biol.* **18**, 3956-3965.
- Gherzi, R., Trabucchi, M., Ponassi, M., Ruggiero, T., Corte, G., Moroni, C., Chen, C. Y., Khabar, K. S., Andersen, J. S. and Briata, P. (2006). The RNA-binding protein KSRP promotes decay of beta-catenin mRNA and is inactivated by PI3K-AKT signaling. *PLoS Biol.* **5**, e5.
- Guo, Z., Zheng, L., Xu, H., Dai, H., Zhou, M., Pascua, M. R., Chen, Q. M. and Shen, B. (2010). Methylation of FEN1 suppresses nearby phosphorylation and facilitates PCNA binding. *Nat. Chem. Biol.* **6**, 766-773.
- Irvine, K., Stirling, R., Hume, D. and Kennedy, D. (2004). Rasputin, more promiscuous than ever: a review of G3BP. *Int. J. Dev. Biol.* **48**, 1065-1077.
- Lee, Y. H. and Stallecup, M. R. (2009). Minireview: protein arginine methylation of nonhistone proteins in transcriptional regulation. *Mol. Endocrinol.* **23**, 425-433.
- Liu, T., Liu, X., Wang, H., Moon, R. T. and Malbon, C. C. (1999). Activation of rat frizzled-1 promotes Wnt signaling and differentiation of mouse F9 teratocarcinoma cells via pathways that require Galphaq and Galphao function. *J. Biol. Chem.* **274**, 33539-33544.
- Liu, T., DeCostanzo, A. J., Liu, X., Wang, H., Hallagan, S., Moon, R. T. and Malbon, C. C. (2001). G protein signaling from activated rat frizzled-1 to the beta-catenin-Lef-Tcf pathway. *Science* **292**, 1718-1722.
- Logan, C. Y. and Nusse, R. (2004). The Wnt signaling pathway in development and disease. *Annu. Rev. Cell Dev. Biol.* **20**, 781-810.
- Lowry, O. H., Rosebrough, N. J., Farr, A. L. and Randall, R. J. (1951). Protein measurement with the Folin phenol reagent. *J. Biol. Chem.* **193**, 265-275.
- Molenaar, M., van de Wetering, M., Oosterwegel, M., Peterson-Maduro, J., Godsave, S., Korinek, V., Roose, J., Destree, O. and Clevers, H. (1996). XTcf-3 transcription factor mediates beta-catenin-induced axis formation in *Xenopus* embryos. *Cell* **86**, 391-399.
- Moon, R. T., Bowerman, B., Boutros, M. and Perrimon, N. (2002). The promise and perils of Wnt signaling through beta-catenin. *Science* **296**, 1644-1646.
- Moon, R. T., Kohn, A. D., De Ferrari, G. V. and Kaykas, A. (2004). WNT and beta-catenin signalling: diseases and therapies. *Nat. Rev. Genet.* **5**, 691-701.
- Mostaqui Huq, M. D., Gupta, P., Tsai, N. P., White, R., Parker, M. G. and Wei, L. N. (2006). Suppression of receptor interacting protein 140 repressive activity by protein arginine methylation. *EMBO J.* **25**, 5094-5104.
- Ortega, A. D., Willers, I. M., Sala, S. and Cuezva, J. M. (2010). Human G3BP1 interacts with beta-F1-ATPase mRNA and inhibits its translation. *J. Cell Sci.* **123**, 2685-2696.
- Parker, F., Maurier, F., Delumeau, I., Duchesne, M., Faucher, D., Debussche, L., Dugue, A., Schweighoffer, F. and Tocque, B. (1996). A Ras-GTPase-activating protein SH3-domain-binding protein. *Mol. Cell Biol.* **16**, 2561-2569.
- Polakis, P. (2000). Wnt signaling and cancer. *Genes Dev.* **14**, 1837-1851.
- Shevchenko, A., Wilm, M., Vorm, O. and Mann, M. (1996). Mass spectrometric sequencing of proteins silver-stained polyacrylamide gels. *Anal. Chem.* **68**, 850-858.
- Soncini, C., Berdo, I. and Draetta, G. (2001). Ras-GAP SH3 domain binding protein (G3BP) is a modulator of USP10, a novel human ubiquitin specific protease. *Oncogene* **20**, 3869-3879.
- Tanner, S., Shu, H., Frank, A., Wang, L. C., Zandi, E., Mumby, M., Pevzner, P. A. and Bafna, V. (2005). InsPecT: identification of posttranslationally modified peptides from tandem mass spectra. *Anal. Chem.* **77**, 4626-4639.
- Tini, M., Naecem, H. and Torchia, J. (2009). Biochemical analysis of arginine methylation in transcription. *Methods Mol. Biol.* **523**, 235-247.
- Tourriere, H., Gallouzi, I. E., Chebli, K., Capony, J. P., Mouaikel, J., van der Geer, P. and Tazi, J. (2001). RasGAP-associated endoribonuclease G3BP: selective RNA degradation and phosphorylation-dependent localization. *Mol. Cell Biol.* **21**, 7747-7760.
- Weber, S., Maass, F., Schuermann, M., Krause, E., Suske, G. and Bauer, U. M. (2009). PRMT1-mediated arginine methylation of PIAS1 regulates STAT1 signaling. *Genes Dev.* **23**, 118-132.
- Yokoyama, N., Golebiewska, U., Wang, H. Y. and Malbon, C. C. (2010). Wnt-dependent assembly of supermolecular Dishevelled-3-based complexes. *J. Cell Sci.* **123**, 3693-3702.
- Zekri, L., Chebli, K., Tourriere, H., Nielsen, F. C., Hansen, T. V., Rami, A. and Tazi, J. (2005). Control of fetal growth and neonatal survival by the RasGAP-associated endoribonuclease G3BP. *Mol. Cell Biol.* **25**, 8703-8716.